ANHYDROUS PROTON-CONDUCTING POLYMERS

Martin F.H. Schuster and Wolfgang H. Meyer

Max-Planck-Institute for Polymer Research, Ackermannweg 10, D-55128 Mainz, Germany; email: meyer@mpip-mainz.mpg.de

■ **Abstract**   Anhydrous proton-conducting polymers usually consist of a more or less inert polymer matrix that is swollen with an appropriate proton solvent (in most cases, phosphoric acid). An outline of the different materials is provided, with a focus on PBI/H_3PO_4 blends that are currently most suitable for fuel cell applications. Also discussed are alternative concepts for fully polymeric materials, which establish proton conductivity as an intrinsic property using amphoteric heterocycles such as imidazole as a proton solvent. The development of some of the first polymers is described, and the fundamental relations between their material properties and conductivity are discussed. Closely related to this relatively new concept are mechanistic investigations focusing on intermolecular proton transfer and diffusion of (protonated) solvent molecules, the contributions of both transport processes to conductivity, and the dependence of these ratios on composition, charge carrier density, etc. Although the development of fully polymeric proton conductors is inseparably related to mechanistic considerations, relatively little attention has been paid to these concepts in the field of conventional membranes (hydrated ionomers, H_3PO_4-based materials). Consequently, their general relevance is emphasized, and according investigations are summarized to provide a more comprehensive picture of proton transport processes within proton exchange membranes.

INTRODUCTION

Since their development in the 1960s, perfluorinated ionomers have emerged as standard materials for low-temperature fuel cell applications because of their high proton conductivity and their excellent chemical and thermal stability. For decades, no other type of material was found to be competitive, despite intense research and a number of severe limitations impeding an economical and wide-spread application of proton exchange membrane (PEM) fuel cells. Without doubt, the most extensive limitations arise from the fact that these materials are proton-conducting only when hydrated, which results in a maximum operating temperature of ∼100°C that in turn limits activity and CO tolerance of the electrocatalyst. Other drawbacks of this type of membrane are the need of permanent humidification (i.e., of additional peripheral devices), high methanol crossover, and limited mechanical stability.

In addition to these factors, which decrease the total efficiency of the system, the high price, as well as difficult recycling or disposal of the perfluorinated materials, has slowed wide-spread and economical application. Accordingly, a variety of alternative approaches using materials that are cheaper and/or more suitable for higher temperatures have been explored, among which are non-fluorinated ionomers and composite membranes (discussed elsewhere in this volume). This article focuses on polymeric materials in which proton conduction does not depend on the presence of an aqueous phase. In general, there are two fundamental approaches toward such membranes. The first one is simply based on the substitution of the water with another suitable proton solvent that is capable of conducting protons in a similar way at higher temperatures. Phosphoric acid has attracted most attention in this context, but aromatic heterocycles are also promising. A second approach points toward fully polymeric systems that exhibit proton conductivity as an intrinsic property. In principle, these materials consist of an acid-doped proton acceptor (or vice versa) that forms mobile protonic defects (excess protons or proton vacancies, respectively). However, the development of a highly conductive all-solid polymer is far from trivial and requires careful tuning of the polymer's properties.

How Dry Is Anhydrous?

From the practical point of view, fuel cell operation at temperatures well above 100°C without the need of humidification is desired, even if some water might be present under these conditions. However, interpretation of the literature data and comparison with other systems are difficult because the exact composition often is unknown, and materials are often prepared in different ways by different research groups. Thus completely dry materials are much more useful for theoretical considerations. However, preparation is more elaborate, and the materials used are idealized rather than optimized systems. This review addresses both the investigation of the fundamentals of proton transport (carried out on well-defined materials) and more practical research, where a certain fraction of water is tolerated.

MATERIALS

Phosphoric Acid-Based Membranes

The property of phosphoric acid to interact via hydrogen bonds facilitates the preparation of blends with a large variety of polymers. In the case of basic polymers, proton transfer from phosphoric acid to the polymer helps for a wide miscibility of these complexes. However, the miscibility limits of phosphoric acid-polymer blends are often unknown, and some of the systems reported in the literature in reality may be inhomogeneous.

PHOSPHORIC ACID   Phosphoric acid is a weak acid ($pK_a = 2.16$) (1) that melts at 42°C in the pure state and acts as an oxidant at elevated temperatures. With

basic polymers, phosphoric acid undergoes hydrogen bond interactions or proton transfer reactions. In regard to its conductivity, phosphoric acid differs from water and many other solvents in two ways. First, conductivity is remarkably high in the pure state (2). Second, when strong electrolytes (e.g., H_2SO_4) are added, conductivity decreases rather than being improved (3). The first feature is due to the generation of charge carriers by self-dissociation ($5H_3PO_4 = 2H_4PO_4^+ + H_2PO_4^-$ $+ H_3O^+ + H_2P_2O_7^{2-}$, where $H_3PO_4 = 16.8$ M, $H_4PO_4^+ = 0.89$ M, $H_2PO_4^- = 0.43$ M, $H_3O^+ = H_2P_2O_7^{2-} = 0.46$ M at 311 K) (4, 5) and the fact that proton migration almost entirely results from structure diffusion (4). The second feature is also closely related to the transport mechanism. The electrical field of extrinsic charge carriers causes a bias on hydrogen bonds and thus suppresses fluctuations within the dynamical hydrogen bond network (6, 7). Addition of water, however, increases conductivity, which passes through a temperature-dependent maximum at compositions of 45 to 60% of H_3PO_4 (2).

POLYMER COMPLEXES   In the mid-1980s, complexes of basic polymers with phosphoric acid (and sometimes sulfuric acid) were discovered as a new class of proton-conducting materials. Thenceforward, a wide variety of polymers were explored [see reviews by Lassègues et al. (8, 9) and Przyluski & Wieczorek (10)]. However, most of these materials suffer from fundamental limitations such as insufficient chemical stability (e.g., hydrolysis of ethers or amides) or low mechanical stability, especially at higher temperatures and larger amounts of incorporated phosphoric acid. Only a few materials have been characterized at temperatures well above 100°C, and even fewer have ever been tested under fuel cell conditions. In the following, a brief overview on the history and the further development of these materials is presented (see also Table 1). Definitions of abbreviations are given at the end of the text.

PEO   PEO/H_3PO_4 complexes ($x = 0.42$–0.66) were described in 1988 by Donoso et al. (11), who found conductivities of $2.5 \cdot 10^{-4}$ S cm^{-1} at 50°C ($x = 0.42$) governed by segmental motion of the polymer chains. Przyluski et al. (12) reinvestigated these blends covering a wider range of compositions ($0.06 \leq x \leq 2.8$) by means of differential scanning calorimetry (DSC), IR, Vogel-Fulcher-Tamman (VFT), and impedance spectroscopy and found VFT behavior for small x and Arrhenius behavior for larger x. The molar amount of acid per mol of polymer repeating units is described by x. Several numerical data had to be extracted from figures, thus a certain error has to be considered. Przyluski et al. (13) also investigated PMMA/PEO blends containing up to 0.5 H_3PO_4 per PEO repeating unit. PMMA here was considered a reinforcing matrix rather than an active material; however, no details of the morphology were reported. Conductivities reached a local maximum at $x = 0.2$ ($2.7 \cdot 10^{-2}$ S cm^{-1} at 50°C) and passed through a minimum for $x = 0.4$. The performance of an ambient temperature H_2/O_2 fuel cell was about 40 mW cm^{-2} (humidified, $x = 0.3$). The maximum in composition-dependent conductivity corresponded to the eutectic composition of PEO/H_3PO_4

TABLE 1 Preparation and conductivities of H_3PO_4 based polymer blends

System	Sample preparation	Drying proc.	H_3PO_4/ rep. unit	σ/S cm^{-1}	Ref.
PEO	Mix-cast	Dry box, mol sieves	0.42	$3 \cdot 10^{-4}$ (50°C)	11
PEO	Mix-cast (CH$_3$CN)	Vac., 3 d	0.5 1.3	$5 \cdot 10^{-5}$ (50°C) 10^{-3} (90°C)	12
PEO/PMMA	Mix-cast (CH$_3$CN/CH$_2$Cl$_2$)	Vac., 2 d	0.2	$3 \cdot 10^{-2}$ (50°C)	13
PEO/sulfamide/ guanidine	Mix-cast (MeOH, CH$_3$CN)	Vac., 7 d, 20°C	0.25, 5%[a]	$\approx 10^{-5}$ (20°C) $\approx 10^{-4}$ (60°C)	15
PMMA-comb-PEO; sulfamide/guanidine	Mix-cast (H$_2$O)	Vac., 14 d, 60°C	0.5, 5%[a]	$3 \cdot 10^{-3}$ (80°C)	17
[b]PEI	Mix-cast (H$_2$O)	Vac., Δ	0.5	$3 \cdot 10^{-3}$ (100°C)	18
[b]PEI	PEI dialyzed, Mix (MeOH)	Precipitate Isolated, evap.	0.54	$1 \cdot 10^{-4}$ (100°C)	20
[l]PEI	Synthesis: ref. (1) Mix (MeOH)	Precipitate Isolated, evap.	0.49	$3 \cdot 10^{-6}$ (100°C)	20
[l]PEI	Mix (MeOH)	Evaporation	2	$1 \cdot 10^{-3}$ (100°C)	23
c-[l]PEI	Swelling (MeOH/H$_3$PO$_4$)	Evaporation	2	$2 \cdot 10^{-4}$ (100°C)	23
Nylon	Mix-cast (HCO$_2$H)	Vac., 2 d, 60°C	1.8	$1 \cdot 10^{-3}$ (70°C)	24
PAAM	Mix (PAAM+H$_3$PO$_4$ 85%)	Vac., 60°C	2	$8 \cdot 10^{-3}$ (40°C)	25
P4VI	Mix(H$_2$O), evap., press.	Vac., 60°C, 2 d	1.5	$3 \cdot 10^{-3}$ (100°C)	54
PAMA $\cdot$ H$_2$PO$_4^-$	Mix with H$_3$PO$_4$, casting	—	2	$1 \cdot 10^{-2}$ (100°C)	69
PVP	Mix-cast (MeOH)	70°C, Argon	2[b]	$1 \cdot 10^{-3}$ (100°C)	70
PBI	Cast (DMAc) immers. 11 M H$_3$PO$_4$	—	5	$4 \cdot 10^{-2}$ (190°)[c]	26
PBI	Cast (DMAc) immers. n M H$_3$PO$_4$	—	4.5 16	$5 \cdot 10^{-2}$ (165°C)[d] 0.13 (160°C)[d]	37
PBI	Cast (DMAc) immers. 10 h, $\sim$ 80% acid 12 h, 100°C	12 h, 100°C	1.7	$1 \cdot 10^{-4}$ (90°C)	59
PBI	Cast (DMAc) immers. n M H$_3$PO$_4$	—	5	$1.9 \cdot 10^{-2}$ (175°C)	64
PBI	dto. PBI/sPSU-Na (3:1)	—	5	$2.1 \cdot 10^{-2}$ (175°C)	64
POD	Immersion (85%)	—	?	0.11 (83°C)	73
H$_3$PO$_4$	—	—	∞	0.28 (100°C)	2

[a]sulfamide/PEO repeating unit; [b]polyphosphoric acid; [c]$p(H_2O) = 1.5$ bar; [d]80–85% rel. humidity.

mixtures (14), which clearly stated the importance of phase behavior of these blends for conductivity.

Bermudez et al. reported on a PEO/sulfamide blend doped with a few percent of guanidine, which led to the formation of (mobile) proton vacancies (15). At room temperature, the conductivity of the solid PEO-sulfamide (4:1) complex increased by a factor of 200 to 650 upon doping with 1 to 5% guanidine, reaching 10^{-5} S cm^{-1}. However, at temperatures around 70°C, conductivities were almost independent of
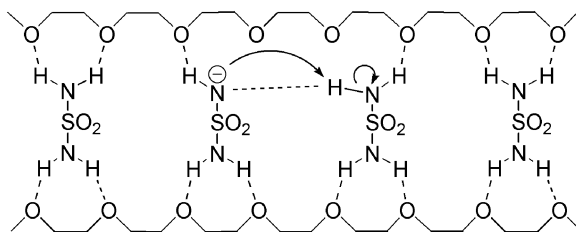
Figure 1 Migration of a proton vacancy defect in a guanidine-doped PEO/sulfamide blend [according to Reference (15)].

the doping level. Infrared (IR) and Raman characterization indicated the (undoped) 4:1 mixture to be well ordered at room temperature (16). To improve thermal and mechanical stability, comb-like PMMA grafted with oligo(ethyleneoxide) side chains was found more suitable than simple PEO/PMMA blends (17). Conductivities were comparable to those in the PEO system (15) under similar conditions; however, at an elevated temperature (80°C), conductivities of $3 \cdot 10^{-3}$ S cm^{-1} were achieved.

In these systems conductivity is established by doping, i.e., a low concentration of extrinsic charge carriers is introduced, and the mechanism is based on proton transport within a rather rigid hydrogen-bonded system, as schematically illustrated in Figure 1. Thus these systems are related to the fully polymeric proton conductors, which are discussed in more detail below.

PEI PEI/H$_3$PO$_4$ blends ($x \leq 0.5$) were introduced by Daniel et al. (18), who found conductivities of 1 to $3 \cdot 10^{-3}$ S cm^{-1} at 100°C. At $x = 0.35$, a precipitate was formed from the aqueous solution, which redissolved upon further addition of H$_3$PO$_4$ ($x = 0.58$). Schoolman et al. (19) characterized blends of higher acid contents ($x \leq 2$) that were applied as electrolytes for electrochromic devices. Whereas these researchers (18, 19) used branched commercial PEI, Tanaka et al. (20) compared branched and linear PEI and found somewhat higher conductivities for the latter; however, compared with the results from Daniel et al. (18), conductivities of the branched materials were about two orders of magnitude lower, which was attributed to the different preparation and purification procedures.

Composition-dependent conductivities of branched and linear PEI blends (18, 20) exhibited a local maximum at $x \approx 0.2$ and dropped to a minimum at $x \approx 0.4$, where the formation of PEI-H$^+$ $\cdot$ $^1/_2$ HPO$_4^{2-}$ was completed (the maximum degree of protonation of PEI is ~80%) (21). This behavior is in accordance with a maximum T_g of the blend (18, 22) and the precipitation from aqueous solution (18) at $x \approx 0.35$. At higher acid levels, conductivity increased again and achieved values of $1.4 \cdot 10^{-3}$ S cm^{-1} (^{l}PEI, $x = 2.05$; 100°C) (23). Properties of the hygroscopic, deliquescent linear PEI blends could be improved by crosslinking,
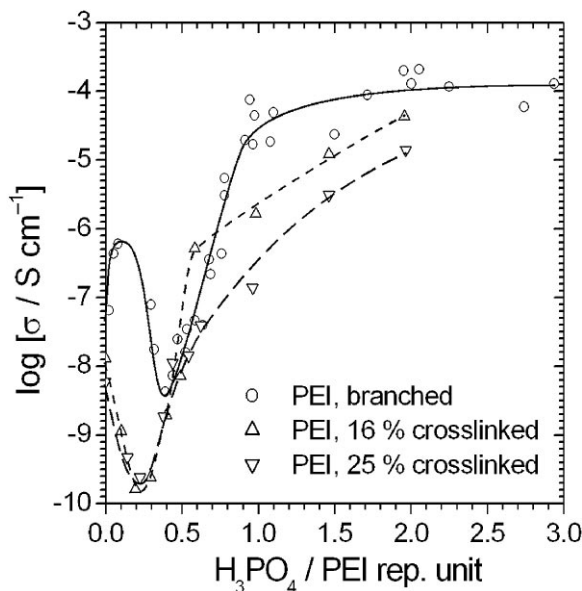
Figure 2 Conductivities of branched and linear cross-linked PEI, respectively, at 50°C as a function of acid content [data taken from Reference (23)].

which moderately influences conductivity at high x, but nearly reverses its dependence on composition at low x (Figure 2) (23). These findings, as well as IR studies (20), indicate that at $x \leq 0.4$, mostly $R_2NH_2^+/R_2NH$ pairs form the basis for proton conduction, whereas at higher x, conductivity is due to an upcoming phase of $H_2PO_4^-$ and H_3PO_4, respectively (Figure 3).

POLYMERS CONTAINING AMIDE FUNCTIONS   A variety of new blends with phosphoric (and sometimes sulfuric) acid have also been investigated. Grondin et al. (24) explored complexes of Nylon® and phosphoric and sulfuric acid, respectively. Conductivities were found to depend little on the type of Nylon (4, 6, 6-6, 6-10). IR experiments indicated hydrogen bond interactions at high temperatures, whereas proton transfer was observed even at very low temperatures, around −180°C. The blends showed no change in IR after two days in air at 100°C; however, their hygroscopic nature caused partial extrusion of the acid at ambient atmosphere. When an amorphous copolymer of a different type of Nylon (El-vamide) was used as a matrix (9), similar conductivities were obtained; however, no mechanically stable films could be formed.

PAAM/H_3PO_4 blends showed relatively high conductivities ($4 \cdot 10^{-3}$ S cm^{-1}, 20°C, $x = 2$). However, condensation of the amide groups was observed at 100°C in dry air (25).
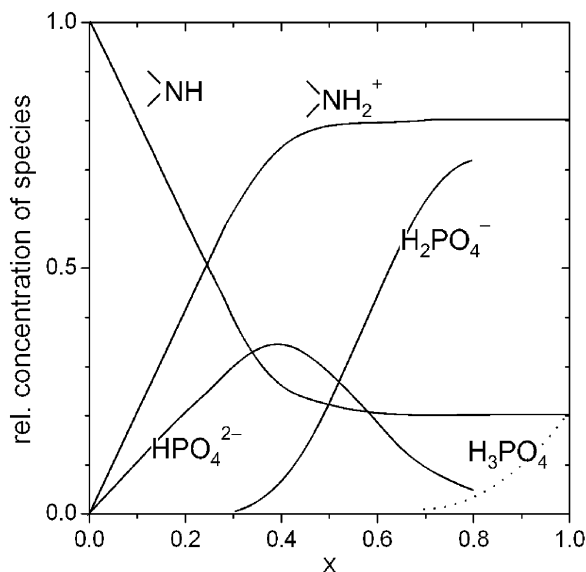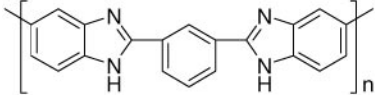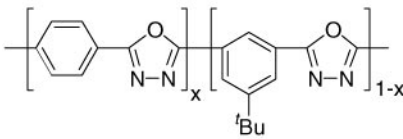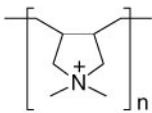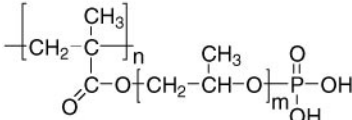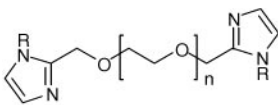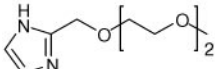
Figure 3 Relative populations of chemical species in PEI/H_3PO_4 blends. The curves have been inferred, rather than calculated, from the large difference between pK_1 and pK_2 of H_3PO_4 and the fact that PEI is only ~80% neutralizable [Reprinted from *Electrochim. Acta* 40(13): 2421–29 with permission from Elsevier (20).]

PBI   In 1995, a blend of poly(benzimidazole) and phosphoric acid was considered for hydrogen fuel cell and direct methanol fuel cell (DMFC) applications for the first time (26). Usually, the term PBI refers to the structure shown in Table 2; however, several related polymers have been prepared (e.g., 27, 28). PBI is an amorphous (29, 30), basic polymer (benzimidazole: $pK_a = 5.5$) (1) of extraordinary thermal stability and a glass transition temperature of about 430°C (29, 31). Conductivities of different PBIs are around 10^{-12} S cm^{-1} in the pure state (e.g., 27, 28). Although all the materials described above suffer from thermomechanical or thermochemical limitations, PBI seems to fulfill the fundamental requirements for fuel cell application.

Compared with the established Nafion^{TM} membranes, PBI is superior in several critical properties. PBI was reported (32) to be about 100 times cheaper than Nafion, and production costs of 150–220 US$/kg for PBI were reported (33), with those for Nafion around 780 US$/m^2 (34). However, at present PBI is exclusively produced by Celanese, who offer only complete membrane electrode assemblies (MEA) for operating temperatures of up to 200°C. Singleton et al. claim a considerably higher mechanical strength of doped PBI than that of Nafion (29, 35). The electroosmotic drag coefficient of water and methanol measured at different water activities, current densities, and temperatures up to 200°C is essentially zero (36, 37), whereas for Nafion, drag numbers of 0.6 to 2 make continuous

TABLE 2 Structures of selected polymers and model compounds

(PBI structure)	Polybenzimidazole (PBI)
(POD structure)	Poly(oxadiazole) (POD)
(PAMA structure)	Poly(diallyldimethylammonium) (PAMA)
(PHP structure)	Phosphonooxyoligo-(ethyleneglycole)methacrylate (PHP)

R = H: Imi-2 ($n = 2$, $T_g = -8\,°C$)
             Imi-3 ($n = 3$, $T_g = -14\,°C$)
             Imi-5 ($n = 5$, $T_g = -24\,°C$)
R = CH$_3$: MeImi-2 ($n = 2$, $T_g = -47\,°C$)

Imi-5/2 ($T_g = -67\,°C$)

humidification essential (38, 39). The methanol permeability is smaller by a factor of about 25 (27, 40). Methanol crossover in different DMFCs was recently reviewed by Heinzel & Barragán (41).

Although the high thermal stability of pristine PBI has long been known— thermogravimetric analysis indicates degradation at 600°C in nitrogen and at ∼500°C in air (42, 43)—Samms et al. confirmed its stability under fuel cell conditions (PBI swollen with H$_3$PO$_4$ and loaded with Pt) (44). Weight loss below 500–600°C was essentially attributed to dehydration (i.e., desorption of residual water and, around 200°C, condensation of H$_3$PO$_4$). However, Musto et al. (45) reported on thermo-oxidative degradation of PBI at 350°C accompanied by only small weight losses (3–5% within 35 h) and in accordance with a mechanism proposed by Conley et al. (46).

Musto et al. (45) also provided tentative assignments of IR absorption bands of pure PBI based on normal coordinate analysis of imidazole and benzimidazole by Cordes & Walter (47) and band assignments from Bellamy (48), indicating both free and self-associated NH functions. The assignment of the NH and CH stretching bands has been verified by comparing pure and partially deuterated PBI films (49). IR studies of blends with HBr, H$_2$SO$_4$, and H$_3$PO$_4$ indicated complete
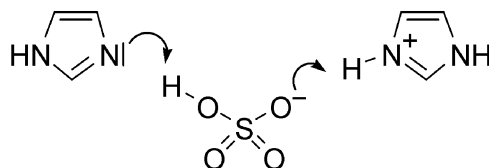
Figure 4 Schematic representation of the proton jump mechanism [according to Reference (49)].

protonation at $x = 1$ for H_2SO_4 (with SO_4^{2-} being the predominant anion for $x \leq 0.6$) and at $x = 2$ for HBr and H_3PO_4 (HPO_4^{2-} was formed only at very small x) (49). Conductivities of all blends were low ($<10^{-11}$ S cm^{-1}) unlike those containing amphoteric species, HPO_4^{2-}, $H_2PO_4^{-}$, and HSO_4^{-}), which were presumed to support a proton transport mechanism (as depicted in Figure 4). IR studies of Glipa et al. (50) confirmed protonation of the imino nitrogen group as proposed by Wasmus et al. (51).

PBI incorporates copious amounts of phosphoric acid even from dilute aqueous solutions (50). While for short immersion times (1 h) the concentration of acid in the liquid phase of the membrane reflects the concentration in the swelling solution, after longer times (16 h), the acid is enriched in the membrane (Figure 5). The
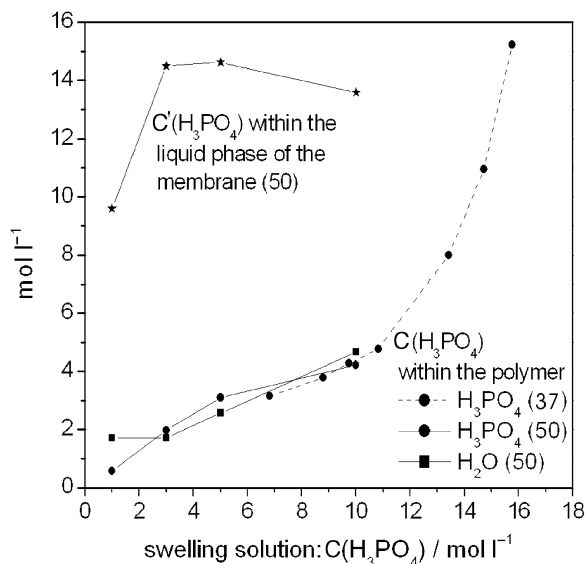

Figure 5 Concentration of H_3PO_4 and H_2O in a PBI membrane and enrichment of H_3PO_4 in the resulting liquid phase after ≥ 16 h of immersion into an aqueous acid solution [data taken from References (37, 50)].

concentration of phosphoric acid in the liquid phase of the membrane $c'_{H_3PO_4} = n_{H_3PO_4} V^{-1}_{liq}$ was calculated from the concentrations of acid $c_{H_3PO_4} = n_{H_3PO_4} V^{-1}_{total}$ and water $c_{H_2O} = n_{H_2O} V^{-1}_{total}$ within the membrane (V_{liq} = volume of the liquid phase, V_{total} = volume of the blend).

Swelling was accompanied by an increase of conductivity and a decrease of mechanical strength (37). Wainright et al. reported that up to five molecules of acid per repeating unit could be incorporated "without adverse effects on the polymer properties" (26), and Li et al. proposed useful compositions to contain 3.5 to 7.5 H_3PO_4 per PBI repeating unit (37).

Figure 6 displays the conductivity data of PBI/H_3PO_4 blends of different compositions prepared by various groups and in different ways. Schechter & Savinell achieved conductivities of $9 \cdot 10^{-3}$ S cm^{-1} at 200°C for blends of PBI (which were cast from trifluoroacetic acid solution) and anhydrous H_3PO_4 (52). Often the preformed PBI membranes were simply immersed into aqueous phosphoric acid of varying concentration. Wainright et al. (26) reported conductivities that increased with the portion of H_3PO_4 and water partial pressure reaching 0.02–0.04 S cm^{-1} at 190°C (pH_2O = 0.5 to 1.5 bar, 5 H_3PO_4/PBI); however, fuel cell resistance
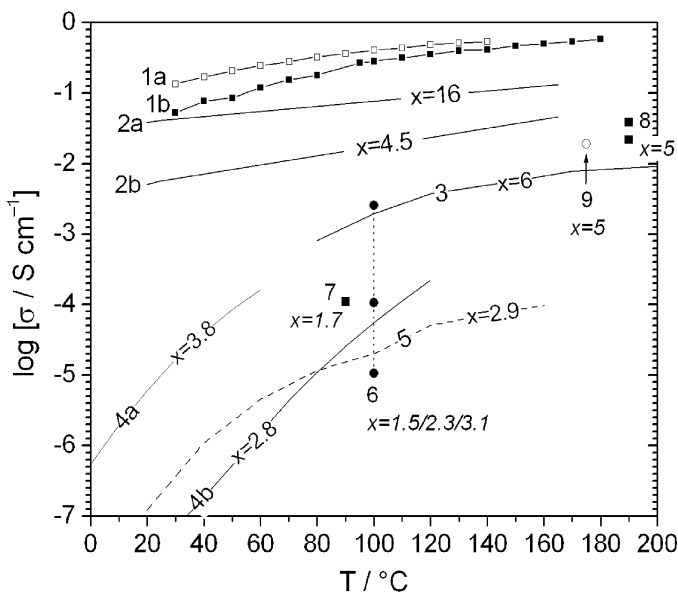
Figure 6 Conductivities of PBI/H_3PO_4 blends prepared by different groups and different methods. (*1a*), H_3PO_4 (1); (*1b*), H_3PO_4 water 80% (1); (*2a + 2b*), PBI/H_3PO_4 water (37); (*3*), PBI/H_3PO_4 99% (52); (*4*), PBI/H_3PO_4 water (61); (*5*), PBI immersed in a H_3PO_4/MeOH solution (94); (*6*), PBI/H_3PO_4, dried (49); (*7*), PBI/H_3PO_4, dried (59); (*8*), PBI/11 M H_3PO_4, upper point: P_{H_2O} = 1.5 bar, lower point: P_{H_2O} = 0.5 bar (26); (*9*), PBI/H_3PO_4 after 50 h at 175°C (56).

was found to be essentially independent of gas humidification (26, 53). At high current densities, fuel cell performance improved slightly upon moderate humidification (53). Li et al. (37) reported even higher values (0.046 S cm^{-1} at 165°C, 4.5 H_3PO_4/PBI and 0.13 S cm^{-1} at 160°C, 16 H_3PO_4/PBI, 80–85% relative humidity).

At relatively high acid contents, conductivities were higher when H_2SO_4 was used instead of H_3PO_4, as already observed for PEI (18, 22), Nylon (24), and P4VI (54). This corresponds to the conductivities of the concentrated aqueous solutions [comprehensive data on solutions of H_3PO_4 and H_2SO_4 are reported in (2) and (55), respectively]. Hasiotis et al. (56) reported that blends of PBI, sPSU [3:1; although not explicitly mentioned, a related article (57) suggests that the sodium form of sPSU was used], and H_3PO_4 exhibited marginally higher conductivities than PBI/H_3PO_4 (0.021 compared with 0.019 S cm^{-1} at 175°C, anhydrous conditions.

Although conductivity of pure sulfuric acid increased by a factor of 7 to 8 upon the addition of imidazole (58), similar attempts failed for phosphoric acid, the conductivity of which decreased by a factor of about 2 upon addition of 10% imidazole (52). Similar results were obtained for PBI/H_3PO_4 blends upon doping with 1-methylimidazole. These findings are in accordance with the observations of Munson & Lazarus (3) and with the proton transport mechanism, as discussed by Kreuer (6, 7).

Conductivity of phosphoric acid-doped PBI was found to decrease with increasing pressure, corresponding to a positive activation volume $\Delta V = -RT \cdot d(\ln \sigma)/dp$. ΔV decreased with increasing temperature and was 4 to 10 cm^3 mol^{-1} between 24 and 90°C (59, 60). Temperature-dependent conductivities followed an Arrhenius law $\sigma(T)T = A \cdot \exp(-Ea/RT)$ with activation energies of 0.74 (61) to 1.08 (59) eV ($p = 1$ bar, 1.7 to 1.8 H_3PO_4/repeating unit), which increased with increasing pressure (59) and increasing amount of acid (61). The activation volume of 85% H_3PO_4 was smaller (becoming negative at higher T) and changed with increasing pressure, showing a positive curvature (60). By comparing PBI/H_3PO_4 blends and hydrated ionomer membranes (62, 63), Fontanella et al. concluded that proton transfer was mediated by segmental motion. Other authors (59, 61) proposed a thermally activated proton transfer within the acidic phase, which was in accordance with the dependence of conductivity on temperature and composition (49), i.e., the high T_g of PBI, and the low ΔV, which was roughly five times smaller than that found in lithium ion transport in polymer electrolytes with typical VTF-behavior.

The performance of PBI/H_3PO_4 membranes in fuel cells (Table 3) appears to be very promising based on the following data: Power densities of 0.1 W cm^{-2} at 200°C for a DMFC (40) and 0.25 W cm^{-2} at 150°C for a H_2/O_2 fuel cell (53) were achieved, and the preparation of the membrane electrode assembly was found to be crucial for the final fuel cell performance. Recently, Li et al. (37) established power densities of 0.55 W cm^{-2} at 190°C without humidification; however, the membranes contained some water from the preparation procedure. At 190°C, 3 vol% CO caused voltage losses of $\approx$0% (0.4 A cm^{-2}) to $\approx$20% (1.2 A cm^{-2}).

TABLE 3 Technical data of PBI-based fuel cells

Preparation	Fuel (humidification)[a]	Catalyst (mg cm^{-2})	Membrane thickness	Power density (W cm^{-2})	Temp. (°C)	Ref.
Cast (DMAc) immers. 11 M H$_3$PO$_4$	H$_2$ (48°C) O$_2$ (28°C)	0.5 Pt	80, 100 μm	0.25 (0.7 A cm^{-2})	150	26, 53
Dto.	MeOH/H$_2$O O$_2$/air (r.t.)	4.0 Pt-Ru 4.0 Pt	80 μm	0.10	200	40
Cast (DMAc) 6.2 H$_3$PO$_4$/PBI	H$_2$ (no) O$_2$ (no)	0.45 Pt	—	0.55 (1.2 A cm^{-2})	190	37
PBI/sPSU-Na Cast(DMAc) immers. 5 H$_3$PO$_4$/PBI	H$_2$/CO (no) O$_2$ (no) MeOH-reformate (r.t.), O$_2$ (no)	0.45 Pt 0.45 Pt	80–110 μm 80–110 μm	0.54 0.47[b] 0.49	200 200	64

[a]Temperature refers to the water the fuel is passed through prior to being fed into the fuel cell.

[b]H$_2$ + 3 vol% CO.

A fuel cell using a polymer blend (75% PBI, 25% sPSU-Na/36% sulfonation, 5 H$_3$PO$_4$ per average repeating unit) achieved 0.54 W cm^{-2} for H$_2$/O$_2$, 0.47 W cm^{-2} for H$_2$ (3 vol% CO)/O$_2$, and 0.49 W cm^{-2} when a methanol reformate was used (200°C, stable within 20 h, residual methanol removed by passing the reformate through water at room temperature, i.e., humidification was low; however, the presence of aqueous H$_3$PO$_4$ was likely) (64). All fuel cells described here were operated at atmospheric pressure.

In addition to hydrogen and methanol, trimethoxymethane (65), formic acid (66), and propane (32) were also tested as fuels for PBI-based fuel cells.

Whether humidification of PBI fuel cells is necessary remains an open question. Short-term fuel cell tests yielded no or small performance losses when dry fuels were used or humidification was reduced (37, 53). However, membrane conductivity does depend on the water activity (26, 67): At 175°C, the conductivity of a PBI membrane (5 H$_3$PO$_4$/PBI) in a dry environment decreased about one third to 0.019 S cm^{-1} within 20 h and remained constant thereafter (>50 h in total). Whether the amount of water produced in a fuel cell is sufficient to maintain a satisfactory performance during long-term operation needs to be clarified. Also, the retention of H$_3$PO$_4$ in such fuel cells still has to be proven under long-term operating conditions.

OTHER THERMOSTABLE POLYMERS The extraordinary properties of PBI have overcome some fundamental limitations of most other polymers previously examined. However, much of the research on anhydrous membranes has focused on PBI, and rarely have alternative polymers been addressed. Alternative thermostable polymers investigated with respect to their proton-conducting properties are P4VI (54, 68), PAMA$^+$H$_2$PO$_4^-$ (69), PVP (70), and POD (71).

At 100°C, the conductivity of P4VI · 1.5 H$_3$PO$_4$ was $3 \cdot 10^{-3}$ S cm^{-1}, whereas the conductivity of PAMA$^+$H$_2$PO$_4^-$ · 2 H$_3$PO$_4$ was $1 \cdot 10^{-2}$ S cm^{-1}. Conductivities of P4VI blended with polyphosphoric acid were about one order of magnitude lower at equivalent compositions and reached $2 \cdot 10^{-3}$ S cm^{-1} at 130°C ($x = 2$).

The PAMA$^+$H$_2$PO$_4^-$/H$_3$PO$_4$ blend (69) is one of the few polymeric proton conductors that has been characterized in detail with respect to the conduction mechanism. ^{1}H and ^{31}P PFG-NMR experiments yielded an increasing $D_{\text{H}}/D_{\text{P}}$ ratio (D = self-diffusion coefficient) with decreasing x, meaning that the incorporation of the acid into the polymer caused a relatively strong immobilization of the former, whereas intermolecular proton transfer was affected to a much lesser extent. Comparison of the self-diffusion coefficients with conductivity data indicates that fast proton transfer processes contribute greatly to conductivity.

Zaidi et al. investigated blends of POD and H$_3$PO$_4$ (85% immersion) exhibiting conductivities as high as 0.11 S cm^{-1} at 83°C (71). The high values were related to the highly porous structure of the membranes, which in turn created poor mechanical properties. These deficits could be improved by compaction, which led to a decrease of conductivity to 0.04–0.07 S cm^{-1}, although conductance improved by a factor of up to three.

NAFION   Savinell et al. reported on a Nafion 117 membrane that was subsequently hydrated and equilibrated with 85% H$_3$PO$_4$ (67). Almost constant conductivities around 0.02 S cm^{-1} were obtained between 100 and 175°C in dry nitrogen. However, no long-term measurements were reported. The performance loss owing to methanol crossover corresponded to a loss of current density of less than 50 mA cm^{-2}. The authors referred to the protonation of phosphoric acid by the super acidic polymer. However, the introduction of charge carriers does not favor high conductivity, at least in the case of pure H$_3$PO$_4$ (3). Consequently, a dependence of conductivity on adsorbed water should be considered, and conductivity might be expected to drop upon prolonged unhumidified operation at temperatures well above 100°C.

Searching for a cheaper material of comparable stability, Sun et al. treated porous Teflon membranes with different surfactants, which caused the material to be swollen with phosphoric acid (85%) (72). Conductivities were around 10^{-3} S cm^{-1} and decreased slightly above 100°C, which might be attributed to a decreasing water fraction.

Blends with Sulfuric and Other Acids

Conductivities of sulfuric acid–swollen PEI (18, 22), Nylon (24), and P4VI (54) were systematically higher compared with those of the phosphoric acid blends. However, x was relatively low (≤ 1) in those cases. The same trend was found for PBI blends (49, 61). However, at $x \geq 1.8$, the H$_3$PO$_4$ blends exhibited higher conductivities (49). Doping with hydrogen halides resulted in low conductivities in all cases [Nylon/HX, X = Cl, Br, I (24) and PBI/HBr (49)].

Other Anhydrous Materials

In addition to the substitution of water as a proton solvent for strong acids, several attempts have been made for other water-free proton-conducting polymer systems. One approach aimed at the swelling of ionomers such as Nafion with *N*-heterocycles as proton solvents. In other approaches, researchers introduced strong proton-donor and proton-solvating functions either by blending two appropriately functionalized polymers or by combining both functions in the same polymer.

NAFION/IMIDAZOLE   In addition to water or phosphoric acid, imidazole may also act as a proton solvent. With respect to its proton-conducting properties (58), Yang et al. used imidazole as a swelling medium for Nafion (73). Conductivity of a membrane cast from a Nafion/imidazole solution was about one order of magnitude lower compared with a fully hydrated Nafion membrane at a given temperature. However, much higher temperatures were accessible for the imidazole-swollen Nafion, reaching the same conductivities as a water-swollen Nafion at about 100 K higher temperatures (Figure 7). It is important to note the dependence of conductivity on preparation: When Nafion was simply immersed into fused imidazole, conductivity was one order of magnitude lower compared with that of a recast membrane, and, at lower temperatures, conductivity broke down, presumably because of imidazole crystallization.

Sun et al. (72) used mixtures of imidazole and 1,2-dimethylimidazole, respectively, with different acids as swelling media for Nafion membranes. Membrane
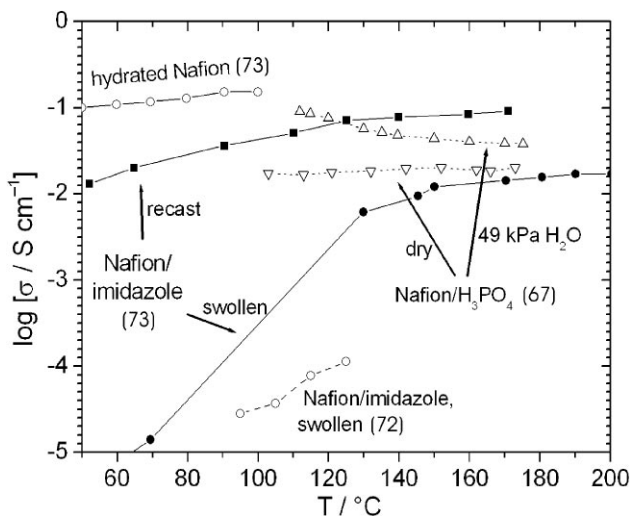

Figure 7   Conductivities of Nafion swollen with water, phosphoric acid, and imidazole, respectively, and those of a recast Nafion/imidazole blend.
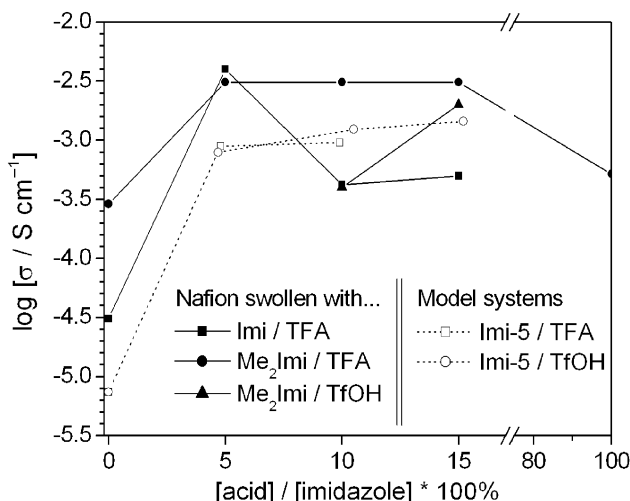
Figure 8   Conductivities of Nafion swollen with acid-doped imidazole derivatives at 100°C. Conductivities of the doped model compound Imi-5 are displayed for comparison [data taken from References (72, 74)].

conductivities were around $4 \cdot 10^{-3}$ S cm^{-1} at 100°C; however, the dependence on concentration and the nature of the acids, as well as the temperature, were quite non-uniform. These results were not easily interpreted owing to the presence of different donor functions, Also, no information on microstructures or exact compositions (e.g., imidazole/Nafion-SO$_3$H) was given.

Figure 8 displays the conductivity data as a function of doping level, and some data regarding an imidazole dimer (Imi-5; Table 2), doped with different acids are included for comparison (74–76). Upon doping, Sun's Nafion/imidazole blends show a strongly increasing conductivity, whereas no further increase is observed at doping levels above 5%. Thus the imidazole derivatives incorporated into the acidic Nafion membrane resemble the behavior of the pristine model compound (Imi-5), i.e., the acidic end groups of the Nafion host do not seem to interact with the imidazole derivatives such that conductivity is favored. Supposedly, immersion does not result in a sufficient solvatization of the SO$_3$H end groups (IR studies could clarify this point). This explanation is also in accordance with the conductivities of the imidazole-swollen Nafion membranes of Sun et al. (72) and Yang et al. (73), which are by far lower compared with that of the recast material (Figure 7).

SULFONIC ACID-BASED MATERIALS   Miyatake et al. (77) reported conductivities of 10^{-3} S cm^{-1} at 150°C for a 1:2 blend of PTPSA and PEO. In a long-term experiment at 130°C, conductivity decreased slightly with time (from 8 to $6 \cdot 10^{-4}$ S cm^{-1} within 100 h, after an initial increase to $1.3 \cdot 10^{-4}$ S cm^{-1}), indicating

the evaporation of loosely bound water. Time-constant conductivity of PTPSA itself was around 10^{-5} S cm^{-1} at 130°C. Deuteration resulted in a 1.4 times lower conductivity (78). The beneficial effect of the high degree of sulfonation (0.85, equivalent weight 210 g/mol) claimed by the authors (77) remains unproven because the conductivities of the hydrated membrane ($>10^{-2}$ S cm^{-1}) resemble the values obtained by Kreuer et al. for a hydrated commercial sulfonated polyetherketone membrane with an equivalent weight of 740 g/mol (58) and because no results for polymer blends with a lower degree of sulfonation were presented.

In a later work (78), the authors stated the insufficient stability of PEO under acidic conditions at high temperatures and reported on an alternative blend using poly(alkylenecarbonates) (PAC) instead of PEO. Conductivities increased when the fraction of PTPSA was increased (PTPSA/PAC = 0.5 to 3 w/w); however, for most samples, changes were small at $1 \leq$ PTPSA/PAC ≤ 3. In spite of careful drying, the residual amount of water was at least 1.4%.

The same authors also reported on a model system containing perfluorooctanesulfonic acid and poly(propylenecarbonate) (PPC), i.e., using a low-molecular weight super acid instead of the polymeric PTPSA that exhibited "a good thermal stability up to 150°C" (79). Conductivities increased upon addition of acid up to a weight ratio of PPC/C$_8$F$_{17}$SO$_3$H = 1:3. At 150°C, conductivities were three times that of the PPC/PTPSA blend (PPC:acid = 1:3 w/w, each). For even higher portions of acid (PPC/C$_8$F$_{17}$SO$_3$H = 1:4 w/w), phase separation was observed and conductivity dropped about two orders of magnitude ($2.5 \cdot 10^{-5}$ S cm^{-1} at 150°C), which resembles the value of the pure acid. Obviously, the presence of protonic defects (which are certainly present in the 4:1 blend) did not suffice for high charge carrier mobility as it occurred in the homogeneous blend. It should be noted that the conductivity of a humid PPC/C$_8$F$_{17}$SO$_3$H sample dropped at $T > 100$°C, whereas the conductivity of a PTMC/PTPSA blend did not (79). Compositions and characteristics of these blends are summarized in Table 4.

TABLE 4   Properties of sulfonic acid–based polymer blends

Sample[a]	Ratio (w/w)	–SO$_3$H/ rep. unit	Drying proc.	Sample prep.	Aspect	Water content	T_g (°C)	$\sigma^{150°\,C}$ (S cm^{-1})	Ref.
PTPSA[b] PEO	1 2	0.10	—	Mix-cast. (MeOH)	Flex., transp., light brown film	$<0.5\%$[c]	5	$1 \cdot 10^{-3}$	77
PTPSA[d] PTMC	3 1	1.5	80°, 5 h, vac.	Mix-cast. (DMSO)	Yellowish, transp. film	$\geq 1.4\%$[c]	9	$1.7 \cdot 10^{-3}$	78
PTPSA[d] PPC	3 1	1.3	80°, 5 h, vac.	Mix-cast. (DMSO)	Yellowish, transp. film	$\geq 1.4\%$[c]	8	$3.3 \cdot 10^{-4}$	78
C$_8$F$_{17}$SO$_3$H PPC	3 1	0.61	80°, 8 h, vac.	Glass wool filter (DMF)	Gel-like, homog.	$\leq 0.5\%$	10	$1.1 \cdot 10^{-3}$	78

[a]M$_W$(PEO) = 600, M$_W$(PTMC) = 5000, M$_W$(PPC) = 77000; [b]85% sulfonation; [c]Karl-Fischer titration; [d]70% sulfonation.

PRISTINE POLYMERS   Rikukawa & Sanui (80) reported moderate conductivities of a graft copolymer bearing phosphate end groups (PHP in Table 2) [m ≈ 6, σ (160°C) = $4 \cdot 10^{-5}$ S cm^{-1}, no humidification]. However, the portion of conductivity that originated from proton migration remained uncertain. On the other hand, Schuster et al. (76) obtained conductivities of $4 \cdot 10^{-6}$ S cm^{-1} (120°C) for a model compound (MeImi-2, Table 2) without dissociating functional groups. The significant conductivity was ascribed to the high mobility of different charge carriers (including impurities) in the viscous material (T_g = −47°C).

Although conductivities of Rikukawa's & Sanui's polymer is low and the methacrylate backbone is unsuitable for fuel cell application, a more detailed characterization could be of interest because the material is quite similar to the fully polymeric proton solvents described below. The low T_g (−75°C) (81) of poly(propyleneoxide), which suggests a high local mobility of the phosphonic acid end groups and the possible introduction of extrinsic charge carriers by doping, should be noted for the following discussion.

Intrinsic Proton-Conductive Polymers

A fundamentally different approach toward high-temperature proton-conducting membranes points to materials with proton conductivity as an intrinsic property, i.e., functioning without any additional liquid phase. Theoretically, the path from a hydrated membrane to a single-phase polymer can be divided into two steps: First, water is substituted with another suitable proton solvent, which, in a second step, is integrated into the material by being covalently tethered to the polymer backbone (Figure 9).

In principle, the second step aims at the immobilization of the proton solvent and thus may also be achieved by coulombic interactions. In this respect, the materials described by Bermudez et al. (15, 17) can be considered as an alternative approach to producing immobilized proton solvents.

THE HISTORY OF POLYMER-BOUND PROTON SOLVENTS   Recently, Kreuer emphasized the proton-conducting properties of nitrogen-containing aromatic heterocycles such as imidazole, pyrazole, and benzimidazole (58, 82). The pure materials exhibited moderate conductivities in the liquid state (82), which was ascribed to
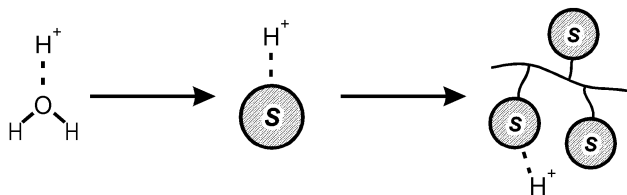

Figure 9   From a hydrated membrane to an immobilized (polymeric) proton solvent S (74).
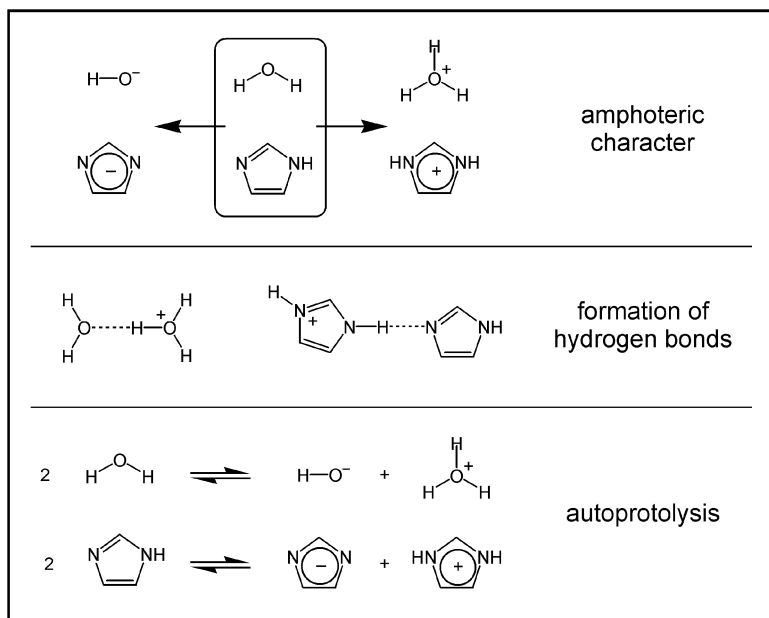
Figure 10   Imidazole and water exhibit similar behavior toward protons (74).

some degree of self-dissociation. In general, the behavior of these materials toward protons is very similar to that of water: The heterocycles are amphoteric molecules; they exhibit extensive hydrogen bond interactions that result in a fluctuating network, and, as mentioned above, to some extent undergo self-dissociation (Figure 10). In addition, they are known for extraordinary thermal and/or chemical stability (83, 84) and have transport coefficients similar to those of water, however, at about 100 K higher temperatures (85).

Of course, phosphoric acid or sulfamide can be discussed in the same way and in principle, this point of view can be applied to any amphoteric molecule. However, not every amphoteric molecule exhibits high proton conductivity, at least in the pure state. One should be aware that proton conductivity owing to a fluctuating hydrogen bond network primarily depends on the rate of these fluctuations rather than on the concentration of intrinsic or extrinsic charge carriers (intrinsic charges carriers arise from self-dissociation and autoprotolysis, whereas extrinsic ones are introduced by the addition of a proton donor or acceptor). The relation between structure, self-dissociation, and proton conductivity was recently discussed by Kreuer (86).

In fact, relatively few materials (e.g., H_3PO_4, imidazole) show considerable conductivities in the pure state on the basis of a relatively high degree of self-dissociation and the formation of a fast-fluctuating dynamical hydrogen bond

network. Due to the adverse effect of extrinsic charge carriers on the conductivity of phosphoric acid (3), protonation by an acidic polymer would be undesirable in this case; instead, a polymer would have to act more or less only as an inert matrix. However, when water, imidazole, or sulfamide is used as a proton solvent, the addition of some extrinsic charge carriers (e.g., acid-doping) is required in order to improve conductivity.

The feasibility of using amphoteric heterocycles as proton solvents was demonstrated by comparing sulfonated PEEK (sPEEK) membranes swollen with imidazole or water, respectively (58). Although the imidazole-swollen materials had to be operated at higher temperatures to achieve conductivities comparable to the hydrated materials, the maximum conductivities were approximately the same. However, at elevated temperatures, pure imidazole evaporated from the membrane just like water. Although the loss of water can be compensated by humidifying the reactants, the evaporation of imidazole cannot be tolerated, and consequently an immobilization of the heterocycles was proposed (Figure 9). Of course, in a material with an immobilized proton solvent, conductivity must be based on proton transfer between the imidazole units and cannot depend on a long-range diffusion of (protonated) solvent molecules. Fortunately, comparison of conductivity data and self-diffusion coefficients indicate that in sPEEK/imidazole (6.7 imidazole/SO_3H) conductivity is predominantly due to intermolecular proton transfer ($D_\sigma/D_{mol} =$ 2.55), where D_σ indicates the mobility of charge carriers, i.e., excess protons or protonic defects, and D_{mol} refers to the molecular self-diffusion of imidazole.

However, tethering imidazole directly to a polymer backbone gave disappointing results: P4VI, as well as several copolymers with 2-acrylamido-2-methylpropanesulfonic acid (P4VI-*co*-AMPS), were prepared (87). In a polymer possessing a high imidazole/AMPS ratio, the heterocycles were expected to provide a migration path for excess protons emerging from the dissociation of the acid functions. However, conductivities of P4VI ($2 \cdot 10^{-11}$ S cm^{-1} at 120°C) and P4VI-*co*-AMPS (10^{-10} S cm^{-1} at 120°C, 5 imidazole/-SO_3H) were very low, which was attributed to the rigid nature of these materials [e.g., $T_g = 210$°C for P($4VI_{2.5}$-*co*-AMPS)]. This is in accordance with the suggestions of Kreuer (82), who proposed that the proton solvent should be bound in a way that suppresses long-range diffusion but still allows high local mobility. Accordingly, flexible spacers were used to tether the proton solvent to the backbone.

In order to systematically identify the parameters governing proton conductivity and its mechanism in this kind of proton conductor, Schuster et al. (74–76) developed a model system consisting of imidazole tethered to oligo(ethylene oxide) chains (Table 2).

The model compounds exhibited considerable conductivities in the pure state owing to self-dissociation of the imidazole units ($5 \cdot 10^{-5}$ S cm^{-1}, Imi-2 at 120°C, compared with $4.6 \cdot 10^{-3}$ S cm^{-1} for imidazole). When small amounts of triflic acid were added as a source of extrinsic charge carriers, conductivities increased by a factor of 50 to reach $2.6 \cdot 10^{-3}$ S cm^{-1} (Imi-2, 0.16 TfOH/imidazole, 120°C). In spite of these fairly low conductivities, important information for the design
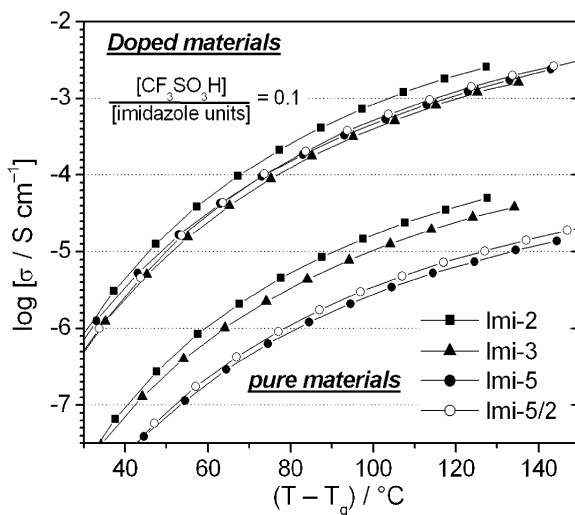
Figure 11   Conductivities of the model compounds Imi-*n* in the pure state and doped with 10% of triflic acid as a function of the reduced temperature [after Reference (74)].

of a polymeric system was obtained. Conductivity was found to depend on the glass transition temperatures and, as expected, on the imidazole volume fraction. However, plotting the temperature-dependent conductivities of the doped materials as a function of the reduced temperature indicates that a low T_g improves conductivity more effectively than a high imidazole volume fraction (Figure 11).

Comparison of conductivity and diffusion data by means of PFG-NMR allowed for a separation of the different contributions to conductivity. Intermolecular proton transfer (structure diffusion) was found to account for more than 90% of the total conductivity at low doping levels (Figure 12). On continued doping, this ratio decreased, a response well known for aqueous acid solutions (88).

The crystal structure of Imi-2 essentially showed an aggregation of the imidazole moieties driven by hydrogen bond interactions (Figure 13). Of particular relevance were the chains formed by the hydrogen-bonded heterocycles, which exhibited a certain similarity to the hydrogen bond network emerging in water and suggested an easy migration of excess protons within these domains. The crystal structure was also in accordance with a possible microstructure, as proposed in Reference (75) (Figure 14).

Goward et al. (89) explored these compounds on a microscopic level using solid-state NMR techniques and found evidence of both rigid and mobile domains. With increasing temperature, an increasing number of mobile protons was observed that were involved in weak, fluctuating hydrogen bonds, thus establishing the basis for structure diffusion. The assignment of chemical shifts to
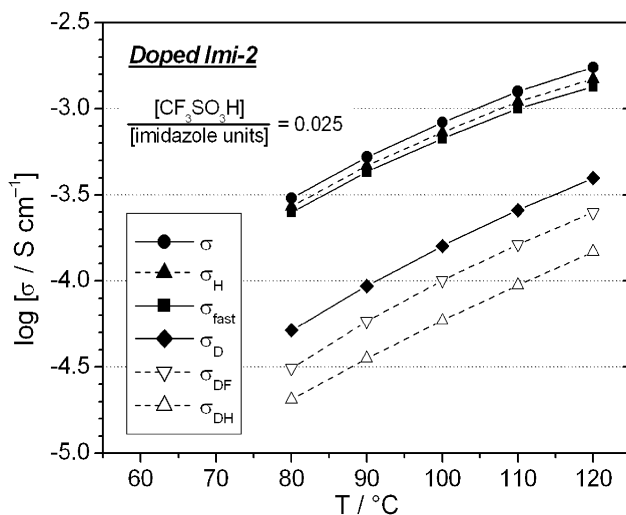
Figure 12 Contributions to the total conductivity σ in Imi-2 doped with 2.5% of triflic acid. σ_{DH}, σ_{DF}, conductivity based on hydrodynamic diffusion (vehicle mechanism) of the protonated Imi-2 and the triflate anion, respectively. $\sigma_D = \sigma_{DH} + \sigma_{DF}$. σ_H, total protonic conductivity ($\sigma - \sigma_{DF}$). σ_{fast}, intermolecular proton transfer ($\sigma_H - \sigma_{DH}$) [after Reference (74)].

strongly and weakly hydrogen-bonded NH protons was supported by density functional theory–based chemical shift calculations. As temperature approached the melting point, coalescence of all NH signals was observed, implying the continued existence of both strongly and weakly hydrogen-bonded species in rapid exchange.

Recently, Herz et al. presented two synthetic means of achieving fully polymeric materials, i.e., with polystyrene or polysiloxane architectures (90). Conductivities of $6 \cdot 10^{-4}$ S cm^{-1} at 200°C were obtained for the undoped polystyrene-based material. Although this seems to be far from the performance of Nafion, there is much room for optimization: The incorporation of a small fractional amount of acidic functional groups was expected to result in a significant improvement of proton conductivity (75, 76). However, the materials reported by Herz et al. were subjected to dielectric spectroscopy, as obtained from bulk polymerization or sol-gel process, respectively, so those early data have to be considered with care. Nonetheless, this work has paved the way for a comprehensive investigation of fully polymeric proton conductors.

All these results indicate a close relation between conductivity and T_g, suggesting that the rate of intermolecular proton transfer depends on the available free volume, which in turn governs the local mobility of the imidazole units. This is in accordance with the results of Münch et al. (91), who simulated the intermolecular transfer of a single excess proton in molten imidazole and found that this

process resulted in an extensive rearrangement of the surrounding hydrogen bond pattern (Figure 14).

Tethering to the polymer backbone is not the only way to restrict the mobility of the proton solvent to a local scale, i.e., to keep it retained in the membrane. In principle, two properties are desired: a very low vapor pressure at elevated temperatures and a certain affinity for the membrane in order to prevent diffusional loss (near zero electroosmotic drag does not suffice). For example, ionic interactions that might serve this purpose could be established between a polyelectrolyte host such as PAMA and imidazole bearing an SO_3-terminated side chain.

In a recent cyclovoltammetric study of liquid imidazole/bis(trifluoromethane-sulfonyl)amide mixtures, Noda et al. found oxidation potentials very close to the reduction potential of oxygen gas, however, with a clear stability increase with increasing acid concentration (92). For high acid concentrations, the electrochemical cell was actually operated in the fuel cell mode, in which currents in the mA range were generated (unfortunately the size and separation of the working and counter electrode were not disclaimed).

Charge carrier mobility can be based either on a distinct liquid phase (water, H_3PO_4, imidazole melt, etc.) or on flexible polymer segments bearing acidic or basic groups. As yet, significant proton conductivities have not been established in a rigid polymer system of such geometry in which proton transfer occurs by hopping over or tunneling through a potential barrier.

MECHANISTICS

Mechanistic considerations are often disregarded thus basing exploration of new materials on empiricism. For example, bearing in mind the results of Munson & Lazarus (3) and Kreuer et al. (4, 7), the adverse effect of imidazole on the conductivity of PBI/H_3PO_4 blends (52) is not very surprising, and the beneficial effect of the protonation of the H_3PO_4 within a Nafion host (67) seems questionable. Also, a pathway for proton migration in Nafion swollen with ionic liquids (i.e., alkylimidazolium salts) (93) hardly seems conceivable. In contrast, for the improvement of polymers as synthesized by Herz et al. (90), the information that structure diffusion-based conductivity reaches a maximum at a doping level ∼5% for imidazole-based systems (75, 76) is sound. These findings also resemble the results of Bermudez & Sanchez (17), who found conductivity of a guanidine-doped sulfamide/comb polymer proton vacancy conductor to be highest at doping levels around 5%.

Mechanistic information can be obtained by comparison of conductivity and diffusion data as provided by dielectric and PFG-NMR spectroscopy, respectively. Using the Nernst-Einstein relationship $D_\sigma = \sigma k T c^{-1} q^{-2}$ (c = charge carrier concentration, q = charge), the conductivity of a diffusional process can be calculated, or the charge carrier mobility (D_σ) can be obtained from the conductivity. It should be noted that the term charge carrier does not indicate that only anions and cations are diffusing within the bulk (vehicle mechanism) but that protonic defects are

also capable of moving according to a mechanism known from semiconductors, namely the migration of excess protons and proton vacancies by intermolecular proton transfer (structure diffusion).

Charge Carrier Mobility and Molecular Self-Diffusion

Charge carrier mobilities (D_σ) higher than molecular diffusion of the solvent molecules (D_{veh}, for vehicles) indicate that intermolecular proton transfer contributes to conductivity (structure diffusion). In certain cases, the diffusion coefficient of the highly mobile protonic species (D_{fast}) can be estimated from the self-diffusion coefficients obtained from PFG-NMR (e.g., by comparing D_H and D_P of phosphoric acid) (4). Often, D_σ is somewhat lower than D_{fast}, indicating a fraction of protonic motion that does not contribute to conductivity (e.g., because of correlated walk of both anions and cations).

As mentioned above, very few proton conductors have been characterized in this way. Among these are pure phosphoric acid, the PAMA/H_3PO_4 blends, the imidazole model compounds Imi-n, imidazole-swollen sulfonated PEEK, and aqueous acidic solutions (Figure 15, Table 5). Figure 15 displays the factor by which the mobility of protonic charge carriers exceeds the self-diffusion of the vehicles, i.e., by which proton conductivity exceeds the value determined for molecular diffusion. D_{veh} corresponds to $D_{31\text{-}P}$ in the case of H_3PO_4-based systems and to $D_{17\text{-}O}$ in the case of aqueous solutions. The model molecule Imi-n contains far more protons that
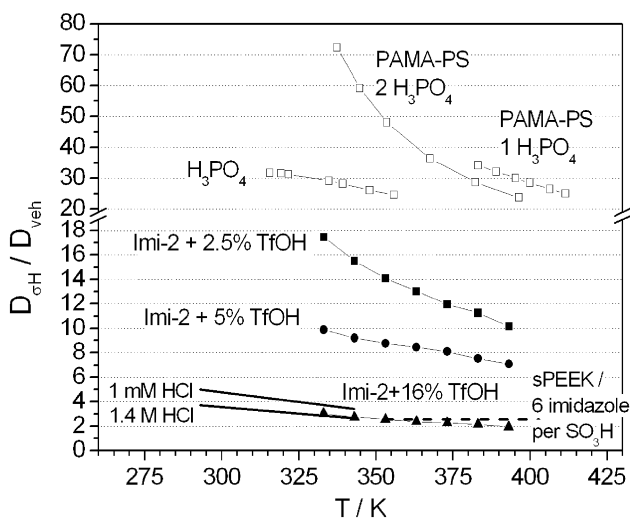

Figure 15 Ratio of protonic charge carrier mobility $D_{\sigma H}$ and self-diffusion of the vehicle molecules D_{veh} for different proton-conducting systems based on phosphoric acid, imidazole, and water, respectively, as proton solvents.

TABLE 5 Nature of proton conductivity in different systems

System	D_{veh}	Doping level (%)[a]	$c(H^+)$ (mol l^{-1})	$D_{\sigma H}/D_{veh}$ (70°C)	σ_{fast}/σ_H (70°C)	Ref.
Imi-2 +2.5% TfOH	D_H	2.5	0.2	15.5	0.94	74–76
Imi-2 + 5% TfOH	D_H	5.4	0.4	9.2	0.89	dto.
Imi-2 + 16% TfOH	D_H	16.4	1.2	2.7	0.63	dto.
H_3PO_4	D_P	—	—	27.2[b]	0.96	4
PAMA$^+$H$_2$PO$_4^-$ · 1 H$_3$PO$_4$	D_P	50	9.5[c]	—	—	69
PAMA$^+$H$_2$PO$_4^-$ · 2 H$_3$PO$_4$	D_P	33	6.3[c]	64	0.98	dto.
sPEEK/imidazole	$D_{H(imi)}$	17	2.5[c]	2.6	0.62	58
Nafion/H$_2$O	D_O	10	5.5[c]	1.3[d]	0.23	85
HCl aq. (1 mmol/l)	D_O	$1.8 \cdot 10^{-5}$	10^{-3}	3.4	0.71	88
HCl aq. (1.4 mol/l)	D_O	0.026	1.4	2.6	0.62	dto.

[a]With respect to imidazole, water, or phosphoric acid; [b]assuming temperature-independent autoprotolysis and self-condensation; [c]with respect to the volume of the liquid phase; [d] at 27°C.

are chemically bound than were added by doping, so in this case D_H essentially represents the molecular diffusion; the anionic conductivity was calculated from $D_{19\text{-}F}$ and was subtracted. Molecular diffusion of imidazole in sPEEK was estimated from D_H by subtracting the significant contribution of intermolecular protons.

Although a significant comparison is hardly possible due to the different nature of the systems (solvent, viscosity, charge carrier density, etc.), two trends are evident. High viscosity (or incorporation into a polymer matrix) impedes molecular diffusion and thus conduction according to a vehicle mechanism, whereas proton transfer processes are affected to a much smaller extent. High charge carrier densities, in contrast, impede intermolecular proton transfer, as discussed above, whereas molecular diffusion is hardly affected. It is interesting to note that the PAMA$^+$H$_2$PO$_4^-$/H$_3$PO$_4$ blends exhibit very high $D_{\sigma H}/D_{veh}$ ratios promoted by the immobilization of the acid phase within the polymer. However, the very high charge carrier densities do not adversely affect the ratio $D_{\sigma H}/D_{veh}$ as one could expect from the results of Munson & Lazarus (3).

The authors note that doping levels (acid/solvent ratio) may correspond to much different charge carrier densities (c_{H+}), depending on the molar volume of the solvent molecules (Table 5). The ratio of protonic charge carrier mobility and molecular diffusion ($D_{\sigma H}/D_{veh}$) is equivalent to the contribution of intermolecular proton transfer to the total protonic conductivity (σ_{fast}/σ_H) according to

$$\frac{D_{\sigma H}}{D_{veh}} = \left(1 - \frac{\sigma_{fast}}{\sigma_H}\right)^{-1}.$$

CONCLUDING REMARKS

In the field of phosphoric acid–based materials, PBI blends currently seem to be unrivaled because all blends using alternative polymers either suffer from inferior stability or, as in the case of POD (71), require optimization of preparation and processing. Unfortunately, research on PBI-based membranes has shifted to a large extent from the academic institutions to industry, and little information on recent developments, fuel cell performance, or long-term stability is available. In addition, after several commercial polymers have been tested with respect to their proton-conducting properties, the exploration of new materials has almost ceased, and the interest of fuel cell researchers focuses on the optimization of fuel cell systems rather than on new membrane materials.

Among the alternative materials, all development regarding single-phase proton-conducting polymers is still in the state of basic research rather than close to application. However, the imidazole-based polymer-bound proton solvents seem promising. Although advanced theoretical knowledge is available, the step from a proof of concept to a stable, optimized membrane remains challenging. Also, new ways of immobilizing low-molecular-weight proton solvents might emerge as a worthwhile option.

Characterization

As discussed in the context of the H_3PO_4-based systems, comparison and evaluation of results is greatly complicated by differing preparation methods and characterization conditions, as well as by poorly defined systems. Improvement of materials' characterization would make comparison with the reported data more valuable. A qualitative description of properties (e.g., transparent, flexible film of moderate tensile strength) and fundamental properties such as T_g would also be helpful. The significance of conductivity and performance data often is limited because it is not clear what the charge transport is based on: Data on the exact composition (e.g., the content of acid and water, or the effect of casting PBI from trifluoroacetic acid) are seldom provided, but even if they are, it is not clear how these variables change during the measurement. In particular, the water content hardly seems to have reached an equilibrium value in some cases, so long-term performance remains uncertain.

Even more important for fuel cell applicability is the question to what extent are the measured conductivities protonic. This is especially true in the case of pure materials such as PHP (80) or Imi-n (74–76), where proton conductivity is strictly subjected to the presence of intrinsic charge carriers (i.e., self-dissociation), and traces of impurities may lead to significant conductivity contributions that do not correspond to proton transport. As mentioned above, MeImi-2 (Table 2) (76) exhibits considerable conductivity, although no intrinsic charge carriers are present (accordingly, these data were used to estimate the effect of impurities). In some cases,

contributions of other ionic species [e.g., low-molecular-weight anions as in the case of the acid-doped model compounds Imi-*n* and in the materials of Sun et al. (72)] must also be considered. For materials such as blends of Nafion and ionic liquids (93), a pathway for proton migration does not seem viable. Consequently, in addition to the conducting properties of a material, the origin and nature of charge carriers must be clarified.

ABBREVIATIONS OF COMPOUNDS

DMAc, *N,N*-dimethylacetamide; P4VI, poly(4-vinylimidazole); PAAM, poly (acrylamide); PAMA, poly(diallyldimethylammonium); PMMA, poly(methyl-methacrylate); PEO, poly(ethyleneoxide); *b*PEI, branched, commercial poly (ethyleneimine), amorphous; *l*PEI, linear poly(ethyleneimine); c-*l*PEI, linear poly (ethyleneimine), crosslinked; PBI, poly(benzimidazole); PHP, phosphonooxyoligo (ethyleneglycol)methacrylate; POD, poly(oxadiazole); PTPSA, poly(thiophenyle-nesulfonic acid); sPEEK, sulfonated poly(etheretherketone); sPSU-Na, sulfonated polysulfone (sodium salt); PEC, poly(ethylenecarbonate); PPA, polyphosphoric acid (*x* refers to average number of phosphate units); PPC, poly(propylenecar-bonate); PTMC, poly(tetramethylenecarbonate).

The *Annual Review of Materials Research* is online at
http://matsci.annualreviews.org

LITERATURE CITED

1. Lide DR, ed. 1995. *CRC Handbook of Chemistry and Physics*. Boca Raton: CRC Press. 76th ed.
2. Chin DT, Chang HH. 1989. *J. Appl. Electrochem.* 19(1):95–99
3. Munson RA, Lazarus ME. 1967. *J. Phys. Chem.* 71(10):3245–48
4. Dippel T, Kreuer KD, Lassègues JC, Rodriguez D. 1993. *Solid State Ionics* 61(1–3): 41–46
5. Munson RA. 1964. *J. Phys. Chem.* 68(11):3374–77
6. Kreuer KD. 1996. *Chem. Mater.* 8(3):610–41
7. Kreuer KD. 2000. *Solid State Ionics* 136–137:149–60
8. Lassègues JC. 1992. In *Proton Conductors: Solids, Membranes, and Gels: Materials and Devices*, ed. P Colomban, pp. 311–28. New York: Cambridge Univ. Press
9. Lassègues JC, Grondin J, Hernandez M, Marée B. 2001. *Solid State Ionics* 145(1–4):37–45
10. Przyluski J, Wieczorek W. 1991. *Synthetic Met.* 45(3):323–33
11. Donoso P, Gorecki W, Berthier C, Defendini F, Poinsignon C, Armand MB. 1988. *Solid State Ionics* 28:969–74
12. Przyluski J, Zalewska A, Maron J, Wieczorek W. 1997. *Polish J. Chem.* 71(7):968–76
13. Przyluski J, Dabrowska A, Stys S, Wieczorek W. 1993. *Solid State Ionics* 60(1–3): 141–46
14. Armand M, Gauthier M. 1989. In *High Conductivity Solid State Ionic Conductors. Recent Trends and Applications*, ed. T Takahashi, Singapore: World Scientific
15. Bermudez VD, Armand M, Poinsignon C, Abello L, Sanchez JY. 1992. *Electrochim. Acta* 37(9):1603–9
16. Bermudez VD, Lucazeau G, Abello L,

Poinsignon C, Sanchez JY, Armand M. 1993. *Solid State Ionics* 61(1–3):219–25

17. Bermudez VD, Sanchez JY. 1993. *Solid State Ionics* 61(1–3):203–12

18. Daniel MF, Desbat B, Cruege F, Trinquet O, Lassègues JC. 1988. *Solid State Ionics* 28:637–41

19. Schoolman D, Trinquet O, Lassègues JC. 1992. *Electrochim. Acta* 37(9):1619–21

20. Tanaka R, Yamamoto H, Kawamura S, Iwase T. 1995. *Electrochim. Acta* 40(13): 2421–29

21. Bloys van Treslong CJ, Staverman AJ. 1974. *Rec. Trav. Chim. Pay-Bas* 93(6):171–78

22. Lassègues LC, Desbat B, Trinquet O, Cruege F, Poisignon C. 1989. *Solid State Ionics* 35(1–2):17–25

23. Tanaka R, Yamamoto H, Shono A, Kubo K, Sakurai M. 2000. *Electrochim. Acta* 45 (8–9):1385–89

24. Grondin J, Rodriguez D, Lassègues JC. 1995. *Solid State Ionics* 77:70–75

25. Rodriguez D, Jegat C, Trinquet O, Grondin J, Lassègues JC. 1993. *Solid State Ionics* 61(1–3):193–202

26. Wainright JS, Wang JT, Weng D, Savinell RF, Litt M. 1995. *J. Electrochem. Soc.* 142(7):L121–23

27. Aharoni SM, Signorelli AJ. 1979. *J. Appl. Polym. Sci.* 23(9):2653–60

28. Pohl HA, Chartoff RP. 1964. *J. Polym. Sci. Polym. Chem.* 2(6):2787–806

29. Singleton RW, Noether HD, Tracy JF. 1967. *J. Polym. Sci. Polym. Symp.* 19:65–76

30. Buckley A, Stuetz DE, Serad GA. 1988. In *Encyclopedia of Polymer Science and Engineering*, ed. HF Mark, 11:572–601. New York: Wiley & Sons. 2nd ed.

31. Gillham JK. 1972. *Crit. Rev. Macromol. Sci.* 1:83

32. Savadogo O, Varela FJR. 2001. *J. New Mater. Electrochem. Syst.* 4(2):93–97

33. Savadogo O. 1998. *J. New Mater. Electrochem. Syst.* 1(1):47–66

34. Barbir F, Gómez T. *Int. J. Hydrogen Energy* 21(10):891–901

35. Wainright JS, Wang JT, Savinell RF, Litt M, Moaddel H, Rogers C. 1995. In *Electrode Materials and Processes for Energy Conversion and Storage*, ed. S Srinivasan, DD Macdonald, AC Khandkar, p. 255. Pennington, NJ: Electrochem. Soc. Proc. Ser.

36. Weng D, Wainright JS, Landau U, Savinell RF. 1996. *J. Electrochem. Soc.* 143(4): 1260–63

37. Li Q, Hjuler HA, Bjerrum NJ. 2001. *J. Appl. Electrochem.* 31(7):773–79

38. Zawodzinski TA Jr, Springer TE, Davey J, Jestel R, Lopez C, et al. 1981. *J. Electrochem. Soc.* 140(7):1981–85

39. Fuller TF, Newman J. 1992. *J. Electrochem. Soc.* 139(5):1332–37

40. Wang JT, Wainright JS, Savinell RF, Litt M. 1996. *J. Appl. Electrochem.* 26(7):751–56

41. Heinzel A, Barragán VM. 1999. *J. Power Sources* 84(1):70–74

42. Belohlav LR. 1974. *Angew. Markomol. Chem.* 40:465–83

43. Jaffe M, Haider MI, Menczel J, Rafalko J. 1992. *Polym. Eng. Sci.* 32(17):1236–41

44. Samms SR, Wasmus S, Savinell RF. 1996. *J. Electrochem. Soc.* 143(4):1225–32

45. Musto P, Karasz FE, MacKnight WJ. 1993. *Polymer* 34(14):2934–45

46. Conley RT, Kane JJ, Ghosh S. 1996. *Tech. Rep.* AFML-TR-71–219

47. Cordes MM, Walter JL. 1968. *Spectrochim. Acta A* 24(9):1421–35

48. Bellamy LJ. 1980. *The Infrared Spectra of Complex Molecules*. Vols. 1, 2. London: Chapman & Hall.

49. Bouchet R, Siebert E. 1999. *Solid State Ionics* 118(3–4):287–99

50. Glipa X, Bonnet B, Mula B, Jones DJ, Rozière J. 1999. *J. Mater. Chem.* 9(12): 3045–49

51. Wasmus S, Daunch A, Moaddel H, Rinaldi PL, Litt M, et al. 1995. Presented at 187th Electrochem. Soc. Meet. Reno. Abstr. 466

52. Schechter A, Savinell RF. 2002. *Solid State Ionics* 147(1–2):181–87

53. Wang JT, Savinell RF, Wainright J, Litt M, Yu H. 1996. *Electrochim. Acta* 41(2):193–97

54. Pu H, Meyer WH, Wegner G. 2001. *Macromol. Chem. Phys.* 202(9):1478–82

55. Darling HE. 1964. *J. Chem. Eng. Data* 9(3):421–26

56. Hasiotis C, Li Q, Deimede V, Kallitsis JK, Kontoyannis CG, Bjerrum NJ. 2001. *J. Electrochem. Soc.* 148(5):A513–19

57. Deimede V, Voyiatzis GA, Kallitsis JK, Li Q, Bjerrum NJ. 2000. *Macromolecules* 33(20):7609–17

58. Kreuer KD, Fuchs A, Ise M, Spaeth M, Maier J. 1998. *Electrochim. Acta* 43 (10–11):1281–88

59. Bouchet R, Miller S, Duclot M, Souquet JL. 2001. *Solid State Ionics* 145(1–4):69–78

60. Fontanella JJ, Wintersgill MC, Wainright JS, Savinell RF, Litt M. 1998. *Electrochim. Acta* 43(10–11):1289–94

61. Pu H, Meyer WH, Wegner G. 2002. *J. Polym. Sci. Polym. Phys.* 40(7):663–69

62. Fontanella JJ, Wintersgill MC, Chen RS, Wu Y, Greenbaum SG. 1995. *Electrochim. Acta* 40(13–14):2321–26

63. Fontanella JJ, Edmondson CA, Wintersgill MC, Wu Y, Greenbaum SG. 1996. *Macromolecules* 29(14):4944–51

64. Li Q, Hjuler HA, Hasiotis C, Kallitsis JK, Kontoyannis CG, Bjerrum NJ. 2002. *Electrochem. Solid-State Lett.* 5(6): A125–28

65. Wang JT, Lin WF, Weber M, Wasmus S, Savinell RF. 1998. *Electrochim. Acta* 43(24):3821–28

66. Weber M, Wang JT, Wasmus S, Savinell RF. 1996. *J. Electrochem. Soc.* 143(7): L158–60

67. Savinell RF, Yeager E, Tryk D, Landau U, Wainright J, et al. 1994. *J. Electrochem. Soc.* 141(4):L46–48

68. Bozkurt A, Meyer WH. 2001. *Solid State Ionics* 138(3–4):259–65

69. Bozkurt A, Ise M, Kreuer KD, Meyer WH, Wegner G. 1999. *Solid State Ionics* 125(1–4):225–33

70. Bozkurt A, Meyer WH. 2001. *J Polym. Sci. Pol. Phys.* 39(17):1987–94

71. Zaidi SMJ, Chen SF, Mikhailenko SD, Kaliaguine S. 2000. *J. New Mater. Electrochem. Syst.* 3(1):27–32

72. Sun J, Jordan LR, Forsyth M, MacFarlane DR. 2001. *Electrochim. Acta* 46 (10–11):1703–8

73. Yang C, Costamagna P, Srinivasan S, Benziger J, Bocarsly AB. 2001. *J. Power Sources* 103(1):1–9

74. Schuster MFH. 2002. *Protonenleitung in imidazolhaltigen Materialien als Modellsysteme für wasserfreie Brennstoffzellenmembranen.* PhD thesis. Univ. Mainz, Germany. 127 pp. (http://ArchiMeD.uni-mainz.de/pub/2002/0017/diss.pdf)

75. Schuster M, Meyer WH, Wegner G, Herz HG, Ise M, et al. 2001. *Solid State Ionics* 145(1–4):85–92

76. Schuster MFH, Meyer WH, Schuster M, Kreuer KD. 2003. *Chem. Mater.* Submitted

77. Miyatake K, Fukushima K, Takeok S, Tsuchida E. 1999. *Chem. Mater.* 11(5): 1171–73

78. Cho JS, Hayashino Y, Miyatake K, Takeoda S, Tsuchida E. 2000. *Polym. Adv. Technol.* 11(8–12):548–52

79. Cho JS, Hayashino Y, Miyatake K, Takeoda S, Tsuchida E. 2000. *Chem. Lett.* (1):44–45

80. Rikukawa M, Sanui K. 2000. *Prog. Polym. Sci.* 25(10):1463–502

81. Gagnon SD. 1985. In *Encyclopedia of Polymer Science and Engineering*, ed. HF Mark. 6:273–307. New York: Wiley & Sons. 2nd ed.

82. Kreuer KD. 1999. In *Solid State Ionics: Science & Technology*, ed. BVR Chowdari, pp. 263–74. Singapore: World Scientific

83. Gelus M, Bonnier JM. 1968. *J. Chim. Phys. Phys. Chim. Biol.* 65(2):253–59

84. Kirsche K. 1994. In *Methoden der organischen Chemie (Houben-Weyl)*, ed. E Schaumann, E8b:401. Stuttgart/New York: Thieme

85. Kreuer KD. 1997. *Solid State Ionics* 97 (1–4):1–15

86. Kreuer KD. 1997. *Solid State Ionics* 94 (1–4):55–62

87. Meister U, Ise M, Kreuer KD, Meyer WH. 1999. Presented at 12th Int. Conf. on Solid State Ionics. Abstr. pp. 429–30

88. Dippel T, Kreuer KD. 1991. *Solid State Ionics* 46(1–2):3–9

89. Goward GR, Schuster MFH, Sebastiani D, Schnell I, Spiess HW. 2002. *J. Phys. Chem. B* 106:9322–34

90. Herz HG, Kreuer KD, Maier J, Scharfenberger G, Schuster MFH, Meyer WH. 2003. *Electrochim. Acta.* Submitted

91. Münch W, Kreuer KD, Silvestri W, Maier J, Seifert G. 2001. *Solid State Ionics* 145 (1–4):437–43

92. Noda A, Susan MABH, Kudo S. Mitsushima S, Hayamizu K, Watanabe M. 2003. *J. Am. Chem. Soc.* Submitted

93. Doyle M, Choi SK, Proulx G. 2000. *J. Electrochem. Soc.* 147(1):34–37

94. Kawahara M, Morita J, Rikukawa M, Sanui K, Ogata N. 2000. *Electrochim. Acta.* 45(8–9):1395–98
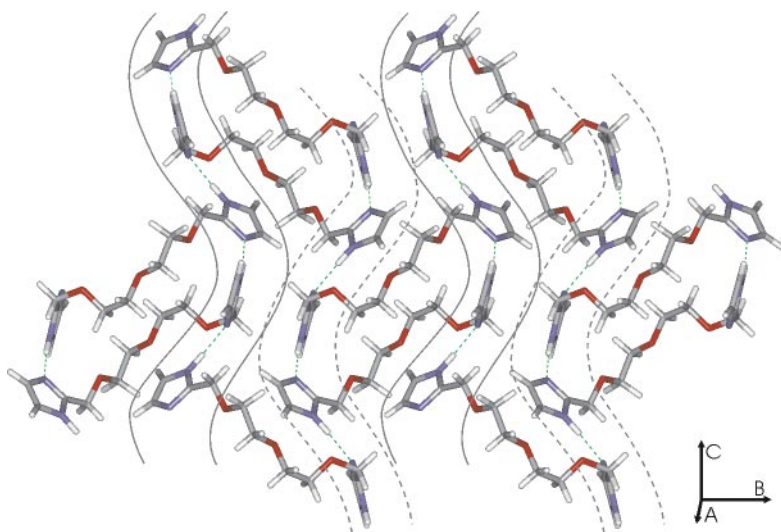
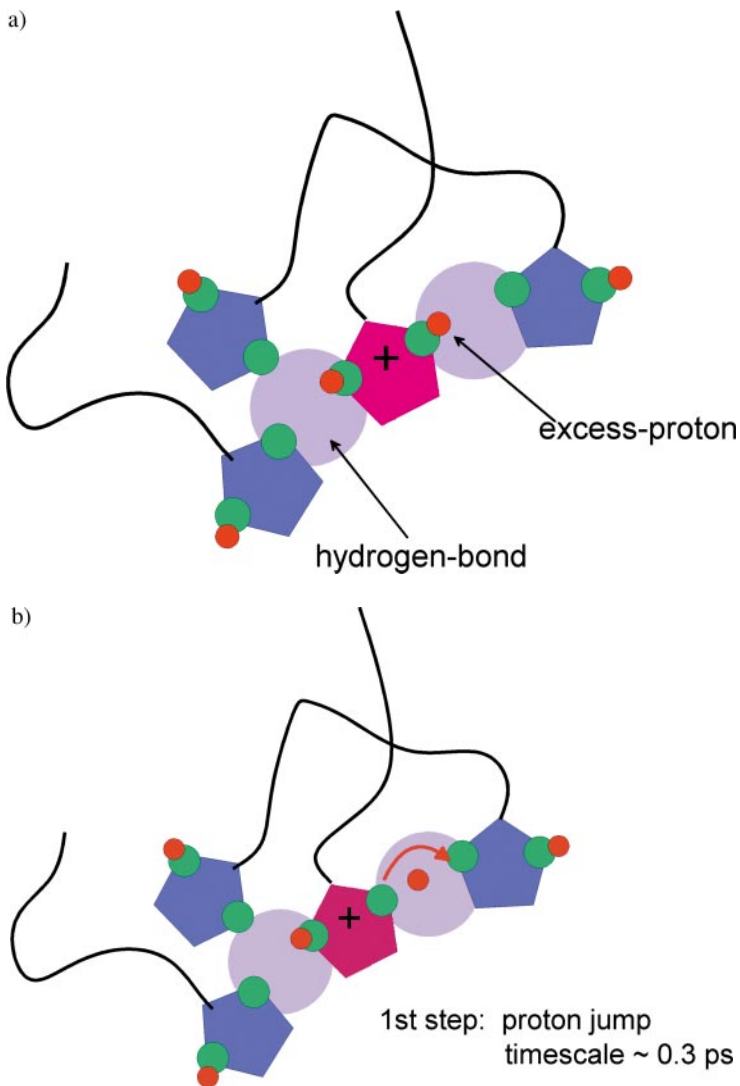**Figure 13**   Crystal structure of Imi-2 (after Reference 74).

a)

excess-proton

hydrogen-bond

b)

1st step: proton jump
timescale ~ 0.3 ps

Figure 14 Schematic of hydrogen-bonded imidazole units and the motion of protonic charge (data from Reference 91): (*a*) starting situation; (*b*) first step: proton jump via hydrogen bond, timescale ∼0.3 ps; (*c*) second step: reorganization of the hydrogen bond pattern via ring rotations and other local dynamics, timescale ∼30 ps; (*d*) final situation.
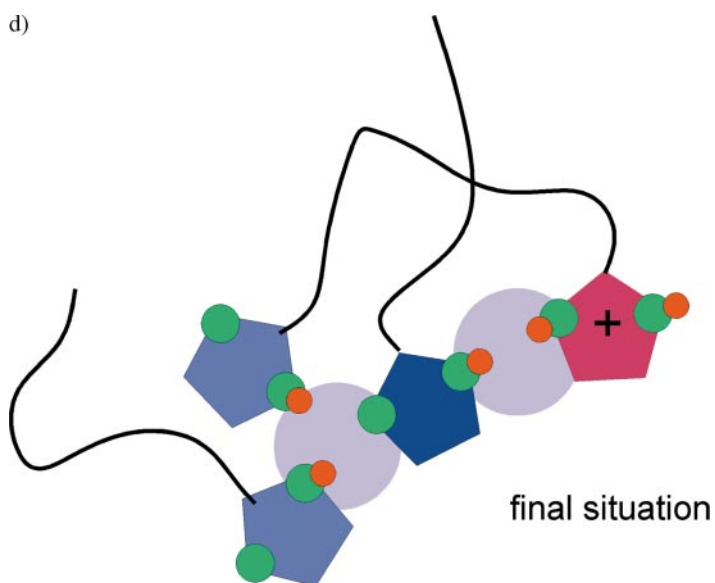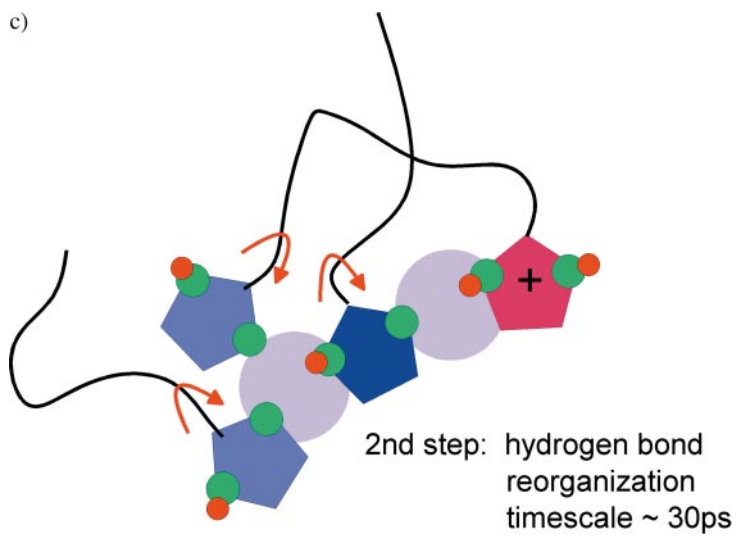
c)

2nd step: hydrogen bond
reorganization
timescale ~ 30ps

d)

final situation

Figure 14   (*Continued*)